The Mortality and Medical Costs of Air Pollution: Evidence from Changes in Wind Direction

Tatyana Deryugina, Garth Heutel, Nolan Miller, David Molitor, and Julian Reif

ONLINE APPENDIX

February 2018

Source of identifying variation

One key advantage of our empirical strategy is that it estimates the impact of pollution on health over a broad geographic area without requiring a detailed "case study" of each individual location. However, this naturally raises questions regarding the ultimate source of our identifying variation. In this section, we illustrate the variation in pollution that drives our results and explicitly test for concerns that may arise when using variation in pollution without specifying the pollution source.

To illustrate the relationship between wind and pollution for each of our monitor groups, we first estimate the following regression separately for each of the 100 monitor groups described in the main text:

$$\text{PM2.5}_{cdmy} = \sum_{b=0}^{34} \beta_b WINDDIR_{cdmy}^{10b} + f\left(Temp_{cdmy}, Prcp_{cdmy}, WindSpeed_{cdmy}\right) + \alpha_c + \alpha_{sm} + \alpha_{my} + \epsilon_{cdmy}. \quad \text{(A1)}$$

The variables $Temp_{cdmy}$ correspond to temperature bins, while $Prcp_{cdmy}$ and WS_{cdmy} correspond to precipitation and wind speed deciles, respectively, following the definitions in equations (1) and (2) of the main text. The function $f()$ represents all their possible interactions. Likewise, the fixed effects follow equations (1) and (2). Equation (A1) differs from the first stage of the instrumental variable regressions estimated in the main text in three minor ways: (1) to demonstrate the source of our variation in more detail, it employs 10-degree bins for $WINDDIR$ instead of 90-degree bins; (2) because we are interested in the relationship between daily wind direction and daily fine particulate matter, it does not include any leads or lags (which we use in the main paper because our outcome variable is 3-day mortality); and (3) it does not employ county weights. Including more wind-direction bins in our main analysis is impractical due to the large number of additional regressors it generates, though we do perform a robustness check to demonstrate the invariance of our results to more wind direction bins in Table 9.

The large number of control variables included in equation (A1) causes estimation to be impossible for six of the monitor groups (see notes in Appendix Figure A1). This does not occur in the instrumental variable regressions we estimate in the main text because the first stage in those regressions is estimated jointly, not separately for each monitor group. (This forces the estimated coefficients on the control variables to be constant across all groups, which increases statistical power.) While one could estimate a version of equation A1 jointly for all monitor groups, doing so would require us to jointly estimate 3500 coefficients (35 wind direction bins for 100 monitor groups), which is computationally infeasible given the size of our data. Here, our goal is to demonstrate the reasonableness and likely validity of our wind direction instrument beyond the robustness checks we perform in the paper, not to show the exact first stage.

The estimates $\hat{\beta}_b$ are plotted as solid black lines in Appendix Figure A1, along with their corresponding 95 percent confidence intervals. The San Francisco Bay Area in California ("Santa Clara, CA") and the Boston, MA area ("Middlesex, MA") are reproduced in Figures 2 and 3 in the main text.

Our empirical approach raises the concern that a small number of monitors located close to local pollution sources may be driving our first-stage results, while monitors located far from those sources may exhibit no significant relationship between wind direction and pollution. If this is the case, then our estimates of the effect of pollution will be driven by local sources near pollution monitors, resulting in potentially significant measurement error. Because we do not observe pollution sources, we cannot test for this directly. However, we can provide indirect evidence by testing for the presence of outliers and by investigating whether the patterns from our first stage are similar for monitor groups located close together. To that end, we conduct two tests.

In the first test, we split each of our 100 monitor groups into two random subgroups. We then estimate equation (A1) separately for each of these 200 subgroups and compare the subgroup estimates to each other and to the group average. Intuitively, if a handful of monitors located near local sources is driving our first stage, then these estimates should differ significantly from each other. By contrast, if the estimated patterns are driven by non-local transport, then the coefficients should be similar. As Figure A1 shows, for the vast majority of monitor groups, the coefficients for each of the two subgroups (dashed red lines) are qualitatively and quantitatively similar to each other and to the overall group average (solid black line), suggesting that our first stage is not driven by locally-produced pollution measured by a handful of nearby monitors.

In the second test, we first classify monitors into 50 groups instead of 100, using the same classification algorithm (kmeans).[1] We then match each monitor group from the 50-group classification to *all* overlapping groups from the 100-group classification. That is, for each of the 50 groups, we find all monitor groups in the 100-group set that have at least one monitor in common. Each of the 50 groups overlaps with 3 to 7 groups from the 100-group classification. This is a much more stringent test than the first one because there may be little overlap between monitor groups from these two classifications. Nevertheless, we expect to see similar patterns in the first-stage estimates because these overlapping groups are located close to each other geographically, and air pollution can be carried by the wind for many hundreds of miles.

[1] We have also replicated all of our results with 50 monitor groups (available upon request). All our estimates are very similar, always falling within the confidence intervals of the estimates with 100 monitor groups. Mortality results with 50 monitor groups for our main sample are reported in column (2) of Table 9 in the main text.

Figure A2 shows the estimated wind angle-pollution relationship in each of the 50 groups (solid black line) and the corresponding relationships in the overlapping groups from the 100-group classification (dashed red lines). Intuitively, if the estimated patterns are driven by non-local transport, then the estimated coefficients should be qualitatively and quantitatively similar. Indeed, this is what we see in the vast majority of cases.

Medicare sample and mortality data

The baseline sample used in our analysis consists of all Medicare beneficiaries aged 65-100 and is derived from 100% Medicare enrollment information files for years 1999-2011.[2] These annual files include an observation for each beneficiary enrolled in Medicare for at least one day in that calendar year, whether enrolled in Traditional Medicare (fee-for-service) or Medicare Advantage. The enrollment files report a variety of demographic and enrollment variables, including unique beneficiary identifiers that can be used to link individuals over time; monthly indicators for Medicare eligibility; state, county, and ZIP code of residence based on the mailing address for official correspondence; and exact date of birth, date of death, and gender.

The vast majority of elderly living in the United States are enrolled in Medicare. The *Left Panel* of Appendix Figure A3 compares the size of our baseline Medicare sample to Census estimates of the U.S. population age 65 and over. To aid comparison, we use Census estimates of the resident population on July 1 each year and limit the Medicare sample to beneficiaries who reside in the 50 states and the District of Columbia and who turned 65 before July 1. Over the period 1999-2011, the Census estimates an average of 37.3 million elderly individuals each year, compared to 36.2 million elderly in Medicare. Thus, the Medicare sample covers over 97% of elderly living in the U.S., a share which remains roughly constant over the sample period.

The mortality variables used in our analysis are based on dates of death recorded in the Medicare enrollment files. Medicare's death data come primarily from the Social Security Administration but are augmented based on reviews triggered by hospitalization claims indicating patient death. The annual mortality rates in the Medicare data align closely with mortality rates based on National Vital Statistics death records and Census population estimates, as shown in the *Right Panel* of Appendix Figure A3. While all recorded deaths in the Medicare data are validated, some death *dates* in the data are not validated, in which case they are assigned the last date in the month of death. Because much of our analysis is performed

[2] The Research Data Assistance Center (ResDAC) provides a helpful overview of the Medicare enrollment information files at http://www.resdac.org/training/workshops/intro-medicare/media/3.

at the daily level, we drop individuals who die at any point in the year and who do not have a validated death date flag. This restriction affects less than 2% of the deaths in our sample, and the share of deaths with unvalidated dates diminishes over time (see Appendix Figure A3).

Estimating counterfactual life expectancy

We model counterfactual life expectancies for Medicare beneficiaries by estimating a semi-parametric Cox proportional hazards model.[3] This model assumes that the hazard rate of death for individual i can be factored into two separate functions:

$$h(t_i|x_i,\beta) = h_0(t_i)\exp[x_i'\beta]$$

The hazard rate at time t_i, $h(t_i|x_i,\beta)$, depends on the baseline hazard rate, $h_0(t_i)$, and on a vector of individual characteristics, x_i. The parameter vector β is estimated by maximizing the log partial likelihood function:

$$\ln L(\beta) = \sum_{i=1}^{N} \delta_i \left[x_i'\beta - \ln \sum_{j \in R(t_i)} \exp[x_j'\beta] \right] \tag{A2}$$

where the indicator variable δ_i is equal to one for individuals whose deaths we observe (uncensored observations) and equal to zero otherwise. The risk set $R(t_k) = \{l: t_l \geq t_k\}$ is the set of observations at risk of death at time t_k and consists of all individuals who are alive at that time. Thus, individuals whose deaths we do not observe (censored observations) affect the partial likelihood function only through the terms indexed by j in equation (A2).

Once $\hat{\beta}$ has been obtained by maximizing the log partial likelihood, we nonparametrically estimate the baseline hazard function following Breslow (1972):

$$\hat{h}_0(t_i) = \frac{d_{t_i}}{\sum_{j \in R(t_i)} \exp[x_j'\hat{\beta}]} \tag{A3}$$

The numerator, d_{t_i}, is the number of deaths that occur at t_i. The corresponding baseline survival function is calculated as

$$\hat{S}_0(t_i) = \exp[-\hat{H}_0(t_i)]$$

where $\hat{H}_0(t_i)$ is the cumulative hazard function, calculated as $\hat{H}_0(t_i) = \sum_{\tau=1}^{t_i} \hat{h}_0(\tau)$. The individual-specific survival function, which allows us to calculate life expectancy, can then be estimated as:

[3] We have also estimated fully parametric models that assume survival rates are governed by either the Gompertz or Weibull distributions. Those results are very similar.

$$\hat{S}(t_i|x_i,\hat{\beta}) = \hat{S}_0(t_i)^{\exp[x_i'\hat{\beta}]}$$

In practice, the nonparametric estimate of the baseline hazard function is limited to the ten years of Medicare data we have available for this survival analysis. We extrapolate the baseline hazard function to future years by assuming it follows a log-linear form. As shown in Appendix Figure A4, this appears to be a very reasonable assumption.

We estimate the Cox proportional hazards model (A2) using data from the 2002 cohort of Medicare beneficiaries, which we observe beginning on January 1st, 2002. We observe all deaths that occur among this cohort on or before December 31, 2011. During this 10-year time period, 50 percent of our sample dies; the remaining deaths are censored.[4] To ensure that we have accurate measures of beneficiaries' chronic conditions, we limit the sample to Medicare beneficiaries who as of January 1, 2002 had been continuously enrolled in fee-for-service Medicare for at least two years. For computational ease, we further limit the analysis to a random 5 percent sample of these beneficiaries. The final estimation sample consists of 1,211,585 individuals.

The life-years lost analysis presented in the main text varies the set of individual characteristics included in the vector x_i in order to understand how they affect the results. As described in the text, we estimate the survival model several times, using increasingly large sets of characteristics. Column (2) of Table 4 includes no characteristics; column (3) includes age and sex, and column (4) includes age, sex, and indicators for 27 different chronic conditions. As we describe in detail below, column (5) utilizes a machine learning algorithm to optimally incorporate information from 1,062 variables. Including so many control variables creates two challenges. First, some variables may be significant predictors of survival for the 2002 cohort just by chance, even if they are not good predictors of survival in general. This may cause bias due to overfitting (Harrell et al. 1996). Second, computational limitations prevent us from including a large set of regressors when performing conventional maximum likelihood estimation on a large sample using standard numerical procedures.

Recent advances in machine learning techniques help us overcome these challenges and use all 1,062 variables when predicting individual-level life expectancies (Athey and Imbens 2016). One popular method is the Least Absolute Shrinkage and Selection Operator (LASSO) estimator (Tibshirani 1997).[5] LASSO can be implemented by maximizing a penalized version of objective function (A2):

[4] Although earlier cohorts are observable for a longer period of time, we do not use them because the Medicare variables denoting the presence of pre-existing chronic conditions, which are strong predictors of survival, are nonexistent or unreliable in earlier years.

[5] We also used other machine learning techniques like ridge regression and elastic net. The results are very similar.

$$\ln L(\beta) = \left(\sum_{i=1}^{N} \delta_i \left[x_i'\beta - \ln \sum_{j \in R(t_i)} \exp[x_j'\beta] \right] \right) - \lambda \sum_{i=1}^{k} |\beta_i| \quad \text{(A4)}$$

where $|\beta_i|$ is the absolute value of β_i (where β_i is element i of the vector β) and k is the number of included regressors. We select the optimal penalty parameter λ using 5-fold cross validation.[6] We include the following 1,062 regressors (not including omitted categories) when estimating this model of life expectancy:[7]

1. Age in days as of January 1, 2002
2. Indicator variables for sex and for 7 different races
3. Indicator variables for the presence of the following 27 different chronic conditions as of December 31, 2001: acute myocardial infarction, Alzheimer's disease, senile dementia, atrial fibrillation, cataracts, chronic kidney disease, chronic obstructive pulmonary disease (COPD), heart failure, diabetes, glaucoma, hip/pelvic fracture, ischemic heart disease, depression, osteoporosis, rheumatoid arthritis, stroke, breast cancer, colorectal cancer, prostate cancer, lung cancer, endometrial cancer, anemia, asthma, hyperlipidemia, benign prostatic hyperplasia, hypertension, and hypothyroidism
    a. Indicator variables for all pairwise interactions of these 27 chronic conditions
4. Indicator variables for the interaction of 27 chronic conditions with 7 race indicators
5. Indicator variables for the interaction of 27 chronic conditions with sex
6. Indicator variables for 12 quantiles (10, 20, 30, 40, 50, 60, 70, 80, 90, 95, 99, 99.9) of the *beneficiary's* total prior year spending (i.e., spending that excludes payments made by Medicare)
    a. Indicator variables for the same 12 quantiles for each of the following 17 different categories of *total* prior year medical spending: hospice, home health care, hospital outpatient, acute inpatient, other inpatient, skilled nursing facility, ambulatory surgery center, Part B drugs, evaluation and management, anesthesia, dialysis, other procedures, imaging, tests, durable medical equipment, other Part B carrier, Part B physician
7. Indicator variables for various quantiles (listed in parentheses) of the 2001 total annual number of:
    a. Dialysis events (10, 30, 50, 70, 90)

[6] See Simon et al. (2011) for a detailed discussion of the algorithm we employ to implement the Cox proportional hazards estimator with a LASSO penalty term. The efficiency of this algorithm allows us to estimate a survival model with both many regressors and a large number of observations.

[7] Variable names correspond to the descriptions given by ResDAC: http://www.resdac.org/cms-data/files/mbsf/data-documentation

b. Home health visits, hospital outpatient emergency room visits (10, 30, 50, 70, 90, 95)
c. Anesthesia events, hospital outpatient visits, other Part B carrier events, acute inpatient stays, durable medical equipment (10, 30, 50, 70, 90, 99)
d. Part B drug events (10, 50, 70, 90, 99, 99.5)
e. Other procedures events, evaluation and management events, imaging events, hospital outpatient emergency room visits, tests events, Part B physician events (10, 30, 50, 70, 90, 99, 99.5)

8. Fourth-order polynomials in each of 37 different variables that have been merged to the respondent's 5-digit ZIP code of residence. All variables are standardized so that they follow a normal distribution with mean 0 and variance 1. These zipcode-level data are obtained from the 2007-2011 and 2008-2012 American Community Surveys. The variables include data on the following categories (number of variables in parentheses if more than one): travel time to work (2), fraction below the poverty line (3), median household income, aggregate household income, aggregate household social security income, aggregate household retirement income, fraction in labor force, heating fuel sources (3), aggregate number of vehicles, median home value, fraction immigrant, gini index of household income, fraction with less than high school education, median year housing built, fraction on disability (2), fraction with hearing difficulties (2), fractions with vision difficulty (2), fraction with cognitive difficulty (2), fraction with ambulatory difficulty (2), fraction with self-care difficulty (2), fraction with independent-living difficulty (2), fraction with any health coverage, (2)and fraction with private health coverage (2).

The counterfactual life expectancy that forms the basis of the estimate in Column (5) of Table 4 is based on estimating (A4) when including the 1,062 regressors listed above.

The dashed lines in Appendix Figure A5 show the distribution of estimated counterfactual life expectancies for the subsample of Medicare beneficiaries who were used to estimate our survival model. The range of the distribution is wider when the model includes all 1,062 predictors (the dashed black line) than when it includes only age and gender as predictors (the dashed red line). The model based on age and sex corresponds to a typical life table and consists of only 68 $(= (100 - 67 + 1) \times 2)$ values. The maximum and minimum values in this table correspond to life expectancies for a 67-year-old female and a 100-year-old male, respectively. By contrast, the LASSO model generates a much larger set of predictions, some of which lie outside of the range of a basic life table.

The solid lines in Appendix Figure A5 show how the distribution of predicted values changes when it is limited to the subset of beneficiaries who died during the 2002 calendar year. The distribution produced by the model that includes only age and sex—given by the solid red line—shifts to the left because these

decedents are older than the average Medicare beneficiary and thus have below-average life expectancies. The distribution for the LASSO model—given by the solid black line—shifts to the left even more. This indicates that beneficiaries who died within one year of January 1, 2002 were not only older than the average beneficiary in that year, but also they were less healthy than average, as captured by variables like prior medical spending and prior chronic conditions. Accounting for these additional variables reduces (on average) the predicted life expectancies for these Medicare beneficiaries. This demonstrates that the Cox LASSO model that incorporates data from many variables generates predictions that are more accurate than a simple Cox model that accounts only for age and sex.

To further validate these estimates, we perform a similar exercise that incorporates Medicare data from individuals not included in our estimation sample. We first use the estimates from our model to predict life expectancy for Medicare beneficiaries as of January 1 of each calendar year. For each of these years, we then calculate the average life expectancy for all fee-for-service beneficiaries who die during that year ("decedents"). We focus on this group because these decedents form the basis of the life-years lost estimates reported in Table 4.

Appendix Figure A6 displays the results of this exercise. The solid green line, which serves as a baseline, displays our estimate of the unconditional life expectancy (11.6 years) for all Medicare beneficiaries. The solid red line displays the average life expectancy among decedents, as predicted by a Cox proportional hazards model that conditions on age and gender. Because the typical decedent is older than the average beneficiary, the predictions from this model are about 2.5 years lower than the baseline. This is clearly a more accurate prediction, since these decedents by definition died within one year of when their life expectancy was estimated. For the sake of comparison, we also include predictions based on a period life table published by the Social Security Administration. Because that life table also conditions on age and sex, its predictions are nearly identical to those of the Cox model. Finally, the solid black line displays estimates based on the LASSO estimation of the Cox proportional hazards model with 1,062 regressors. This reduces the prediction by yet another 2.5 years. The estimates decline slightly over time, which likely reflects the improvement in the recording of chronic conditions in later years.[8]

[8] Medicare data on chronic conditions become increasingly incomplete in earlier years beginning in 2006. Because beneficiaries in these earlier years are less likely to have their chronic conditions recorded in the data, their estimated life expectancy is higher than beneficiaries in later years, who are more likely to have chronic conditions.

APPENDIX FIGURES

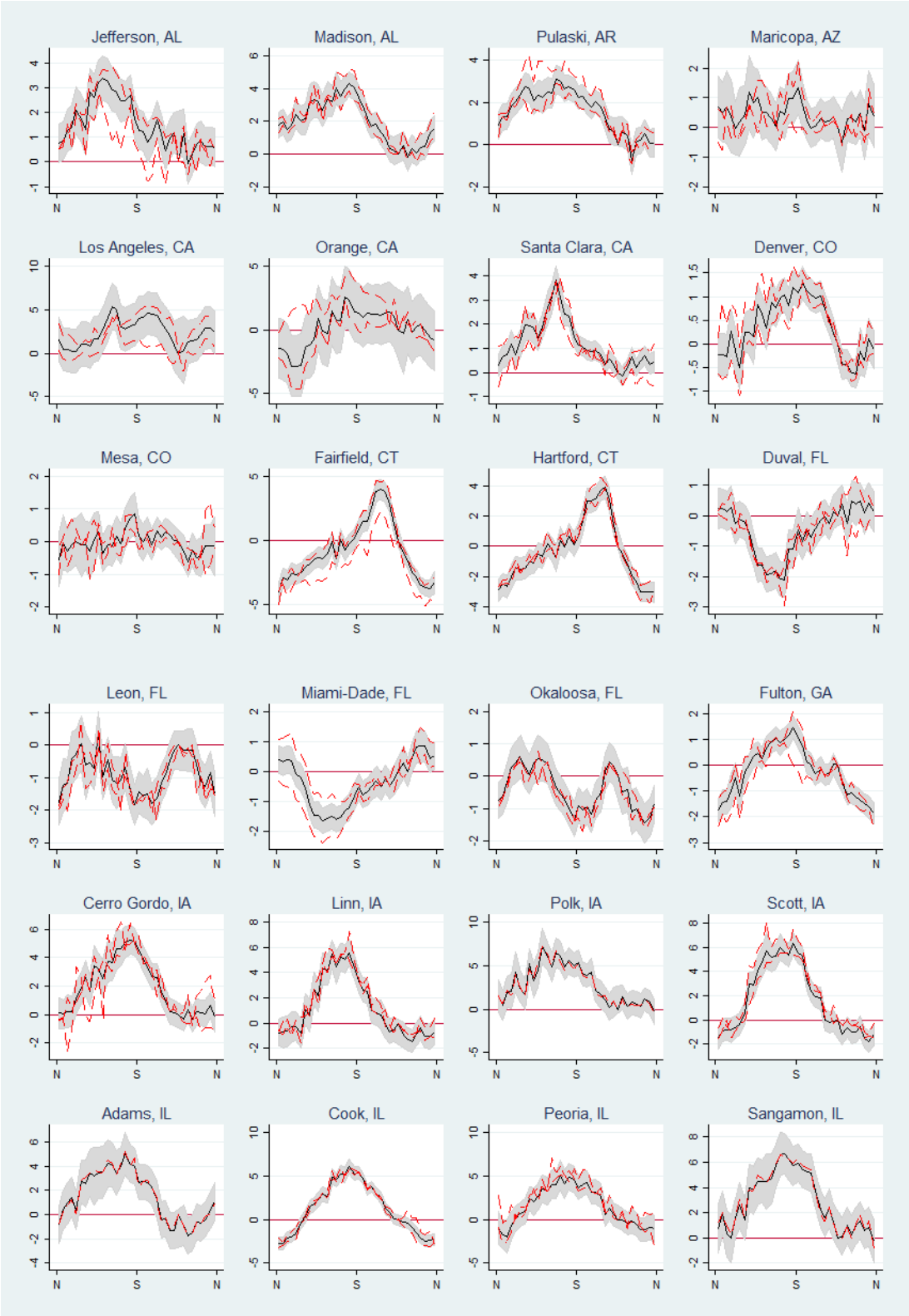

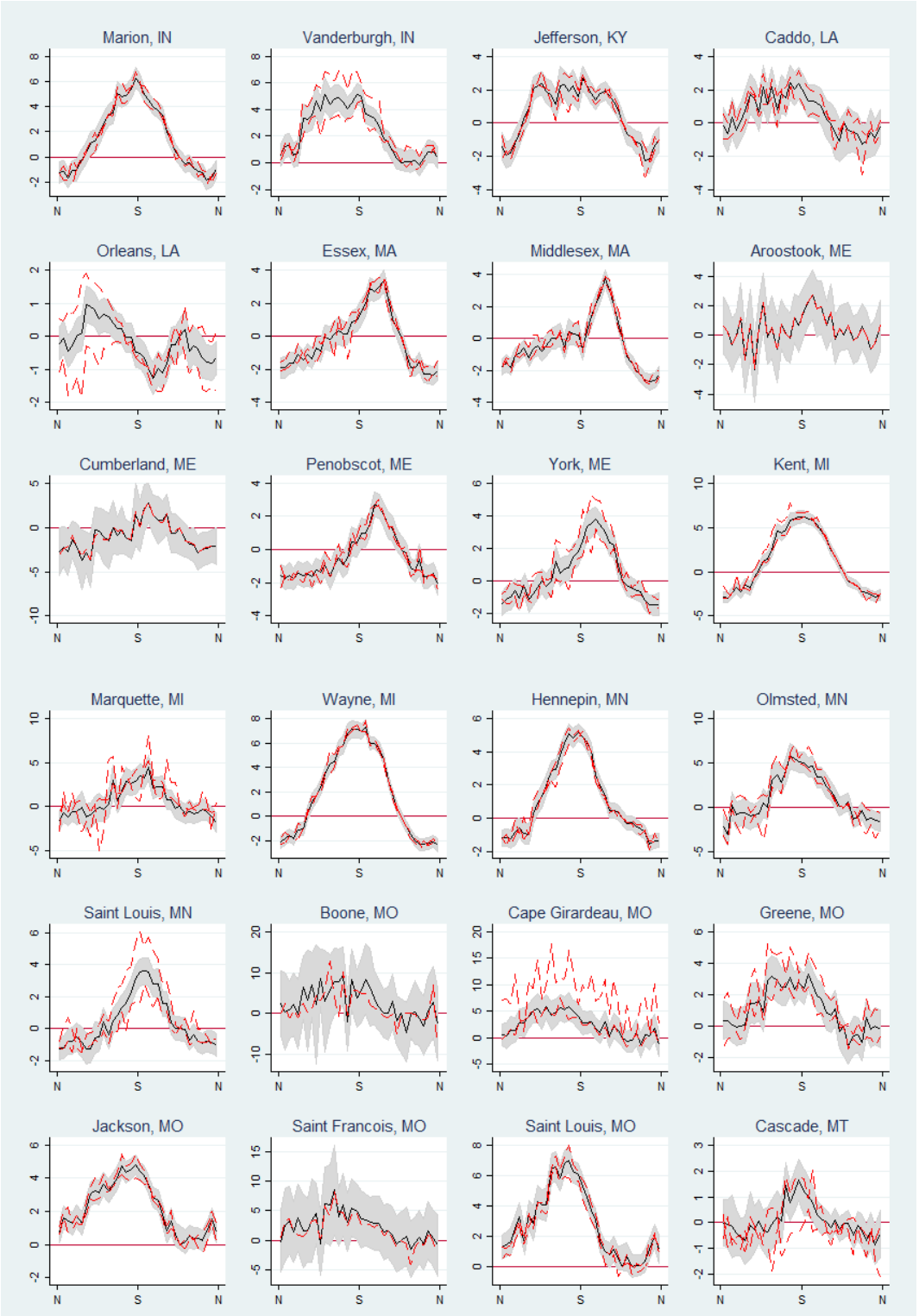
Marion, IN
Vanderburgh, IN
Jefferson, KY
Caddo, LA
Orleans, LA
Essex, MA
Middlesex, MA
Aroostook, ME
Cumberland, ME
Penobscot, ME
York, ME
Kent, MI
Marquette, MI
Wayne, MI
Hennepin, MN
Olmsted, MN
Saint Louis, MN
Boone, MO
Cape Girardeau, MO
Greene, MO
Jackson, MO
Saint Francois, MO
Saint Louis, MO
Cascade, MT
N
S
N

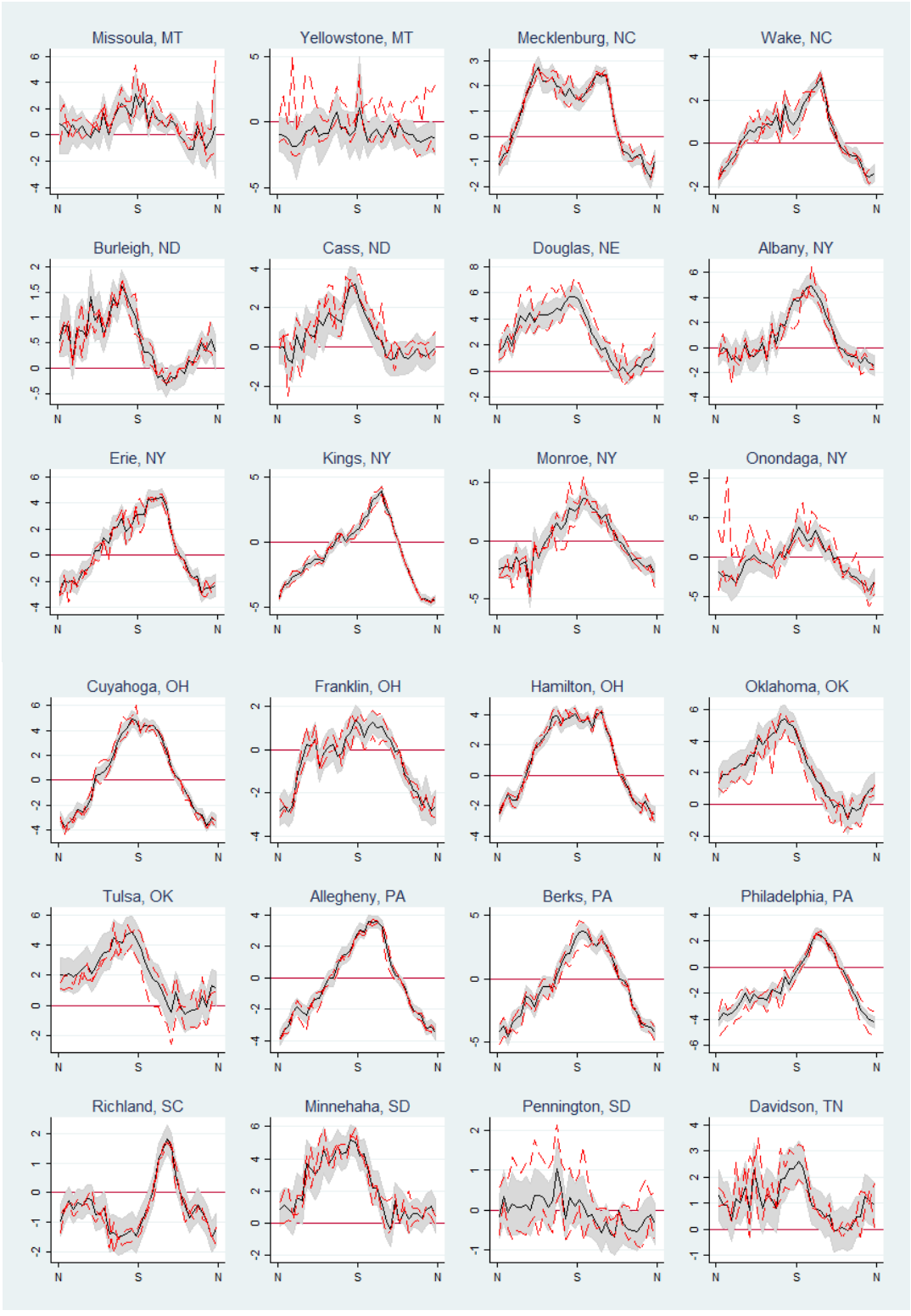
Missoula, MT
Yellowstone, MT
Mecklenburg, NC
Wake, NC
Burleigh, ND
Cass, ND
Douglas, NE
Albany, NY
Erie, NY
Kings, NY
Monroe, NY
Onondaga, NY
Cuyahoga, OH
Franklin, OH
Hamilton, OH
Oklahoma, OK
Tulsa, OK
Allegheny, PA
Berks, PA
Philadelphia, PA
Richland, SC
Minnehaha, SD
Pennington, SD
Davidson, TN
N
S
N

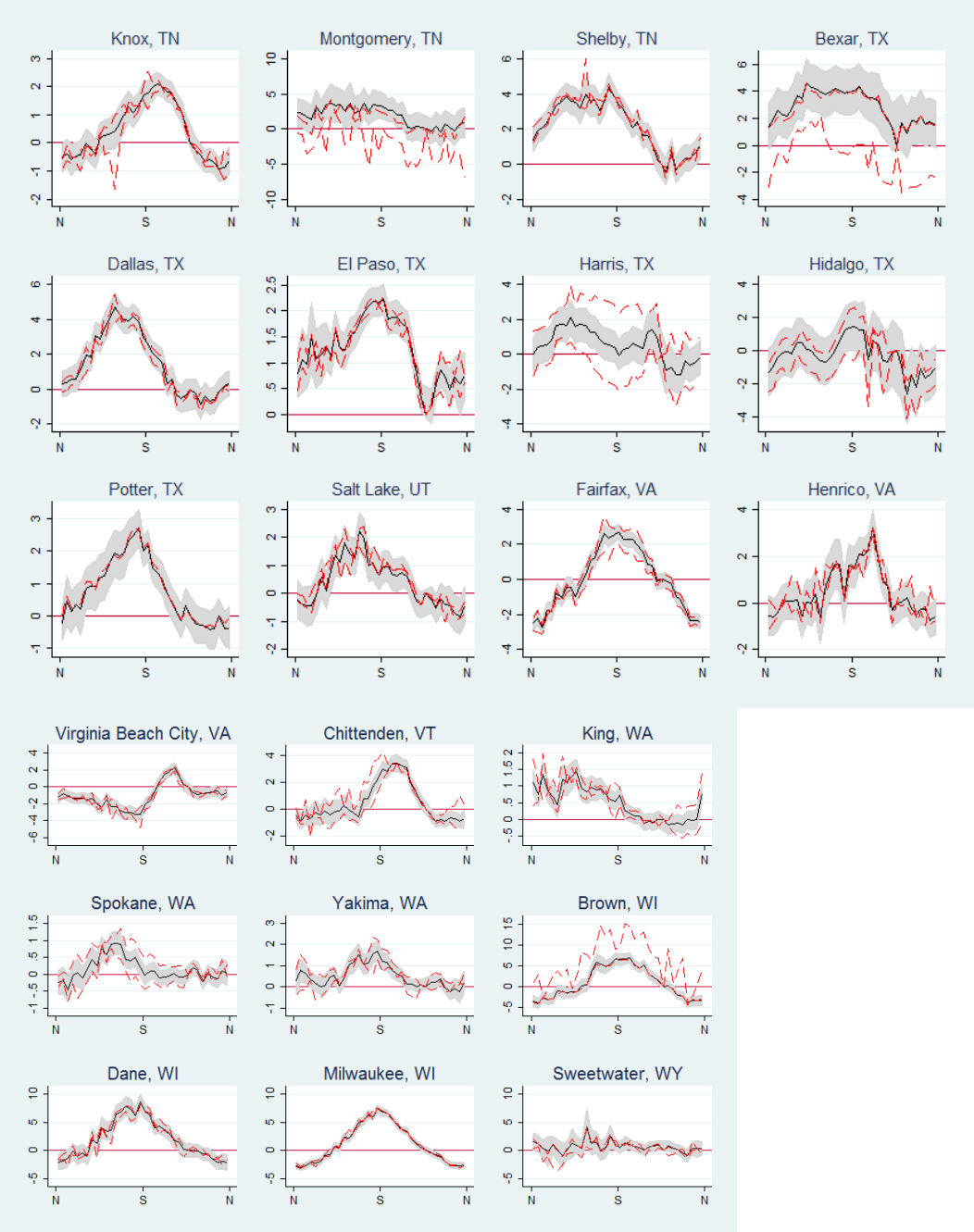

Appendix Figure A1. Relationship between wind direction and PM 2.5 concentrations for each of the 100 monitor groups employed in the main text. Grey area represents the 95 percent confidence interval for the overall estimate (solid black line). Dashed red lines display estimates for two subgroups to which counties in each group were randomly assigned. Graph titles report the most populous county in the group. Graphs are ordered alphabetically by state and county. Six pollution monitor groups with fewer than 1,000 PM 2.5 readings are not shown. Two subgroups are omitted due to insufficient number of observations (one in the Sangamon, IL group and one in the Potter, TX group).

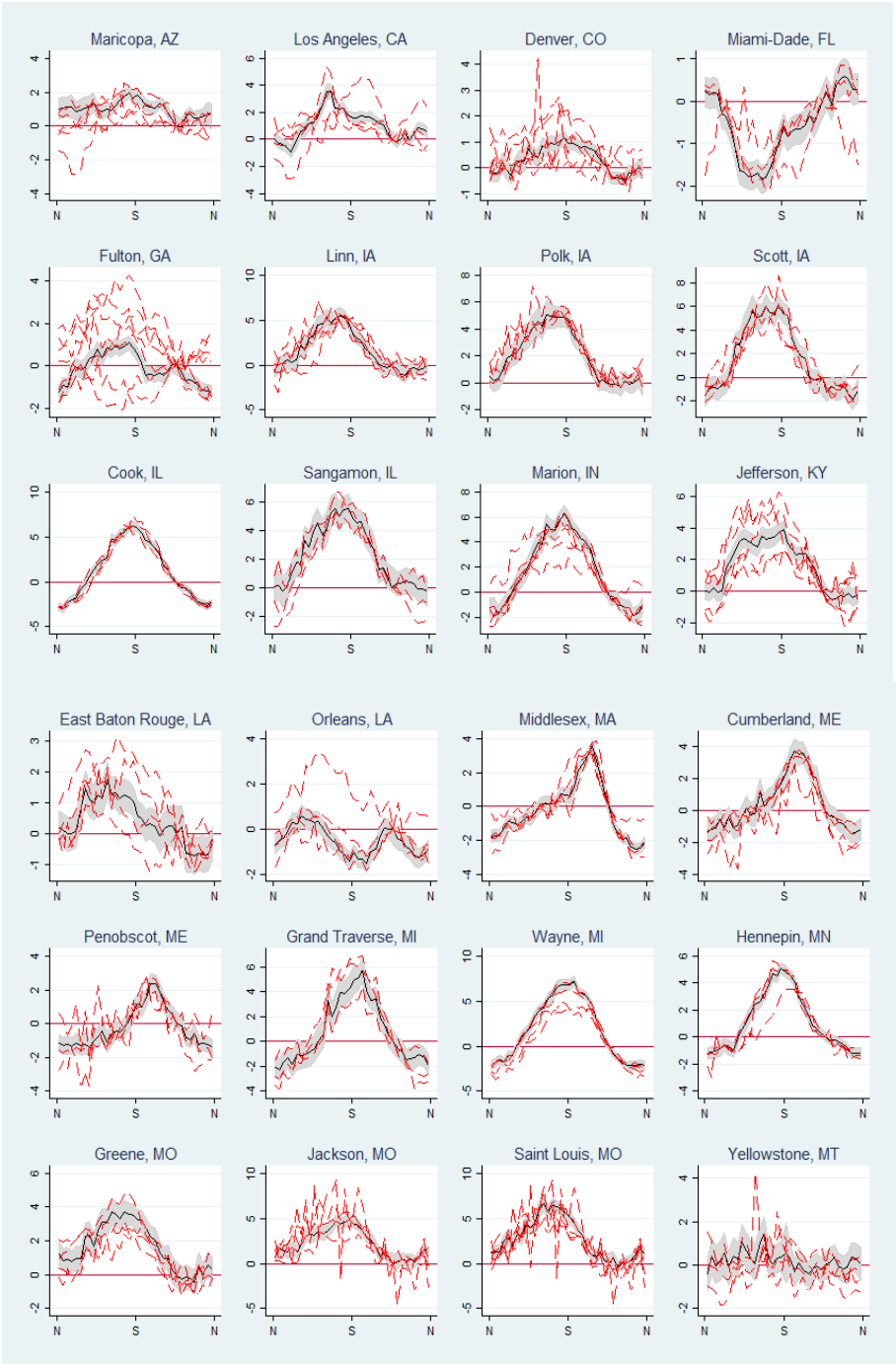
Maricopa, AZ
Los Angeles, CA
Denver, CO
Miami-Dade, FL
Fulton, GA
Linn, IA
Polk, IA
Scott, IA
Cook, IL
Sangamon, IL
Marion, IN
Jefferson, KY
East Baton Rouge, LA
Orleans, LA
Middlesex, MA
Cumberland, ME
Penobscot, ME
Grand Traverse, MI
Wayne, MI
Hennepin, MN
Greene, MO
Jackson, MO
Saint Louis, MO
Yellowstone, MT
N
S
N

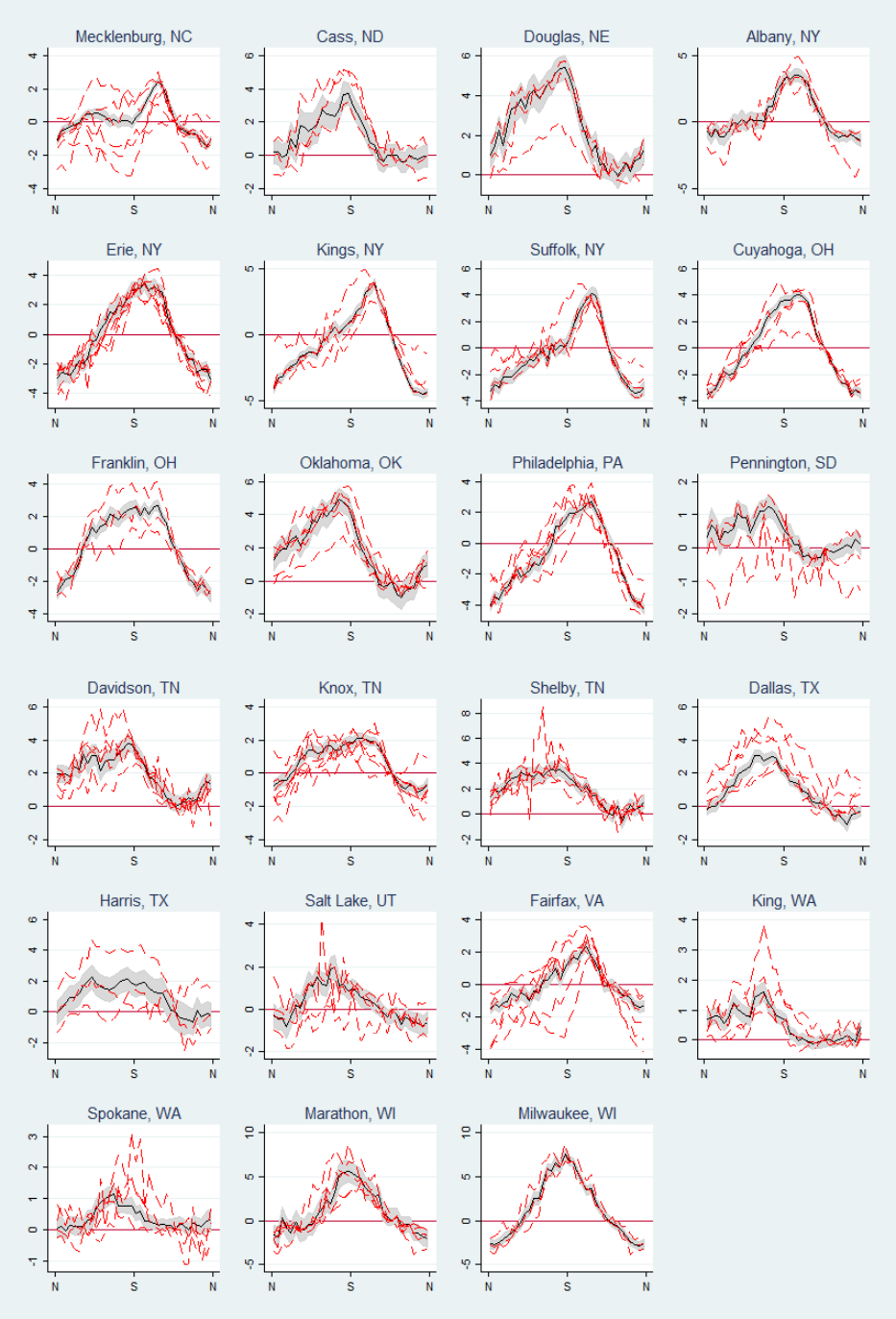

Appendix Figure A2. Relationship between wind direction and PM 2.5 concentrations for each monitor group in the 50-monitor group classification and for corresponding monitor groups in the 100-monitor group classification. Grey area represents the 95 percent confidence interval for the 50-monitor-group estimate (solid black line). Dashed red lines correspond to point estimates for all monitor groups in the 100-monitor-group classification that have at least one monitor in common with the group from the 50-monitor-group classification. Graph titles report the most populous county in the group. Graphs are ordered alphabetically by state and county. Three pollution monitor groups with fewer than 1,000 PM 2.5 readings are not shown.

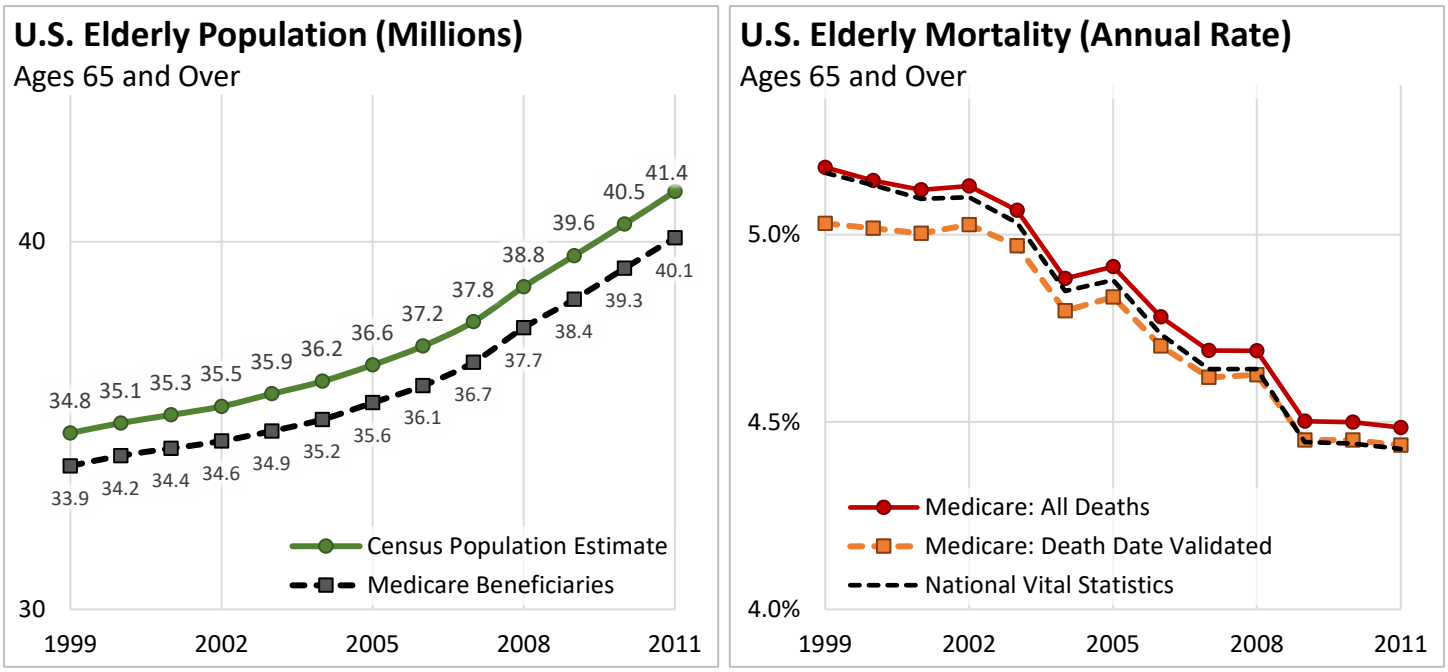

Appendix Figure A3. Population and Mortality Among U.S. Elderly, 1999-2011.

Left Panel: Census population estimates are derived from U.S. Census Bureau files. Estimates for 1999-2009 are intercensal estimates of the July 1 resident population age 65 and over; estimates for 2010-2011 are postcensal estimates of the July 1 resident population age 65 and over. Medicare beneficiaries for a given calendar year include all individuals age 65-100 in the corresponding annual Medicare enrollment file, limited to those who turned 65 before July 1 of the year and have a ZIP code of residence located in the 50 states or the District of Columbia.

Right Panel: National vital statistics mortality data come from the Compressed Mortality File (CMF), which is produced by the National Center for Health Statistics and is based on death certificates filed in the 50 states and the District of Columbia. To obtain vital statistics mortality rates, we divide total CMF deaths among the 65 and over population in a given year by the Census population estimates shown in the *Left Panel*. The dashed lines report annual mortality rates based on death dates recorded in the Medicare annual enrollment files. The figure reports both the total mortality rate in the Medicare sample, as well as the mortality rate among the analytical sample used in the paper which excludes individuals who have a validated death that year but do not have a validated death *date* flag.

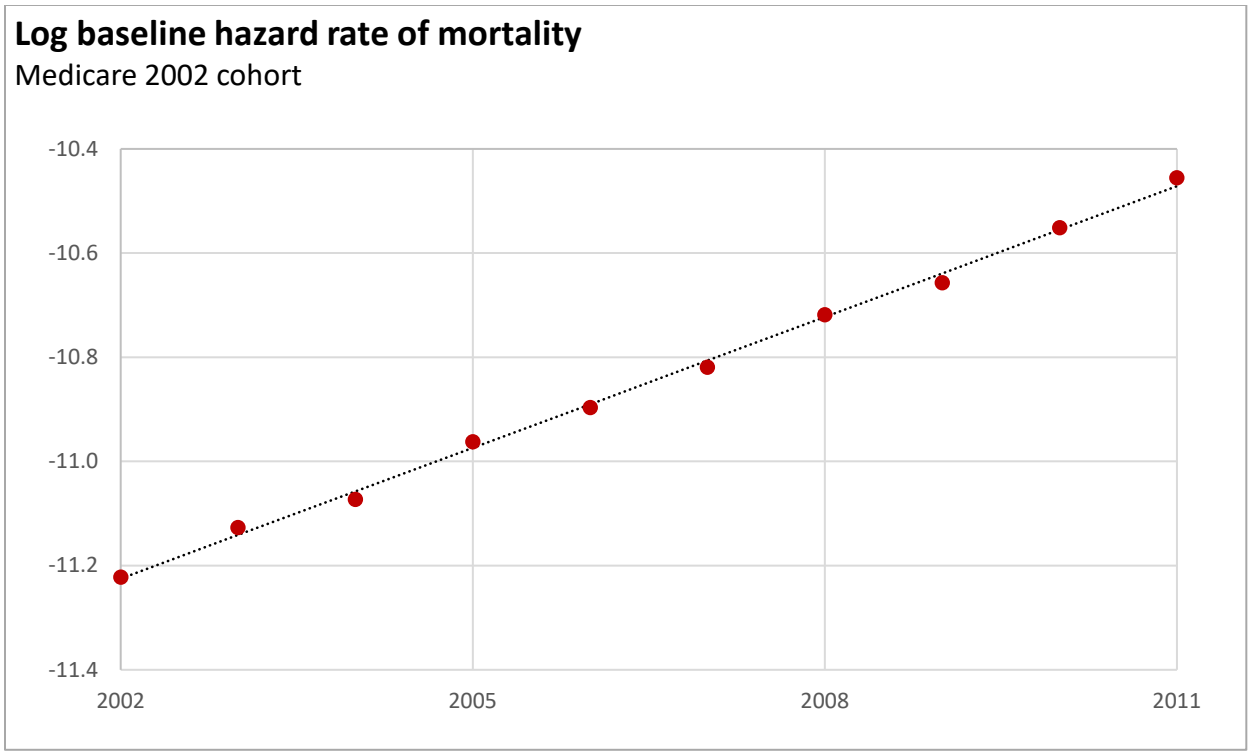

Appendix Figure A4. Log of the baseline hazard rate for the Medicare 2002 cohort. The red points in the figure correspond to the log of the baseline hazard rate of mortality for the Medicare 2002 cohort, as estimated by equation (A3) when using age and gender as controls. The coefficients on age and gender were estimated using the Cox proportional hazards model (A2). The figure also displays a dotted line of best fit.

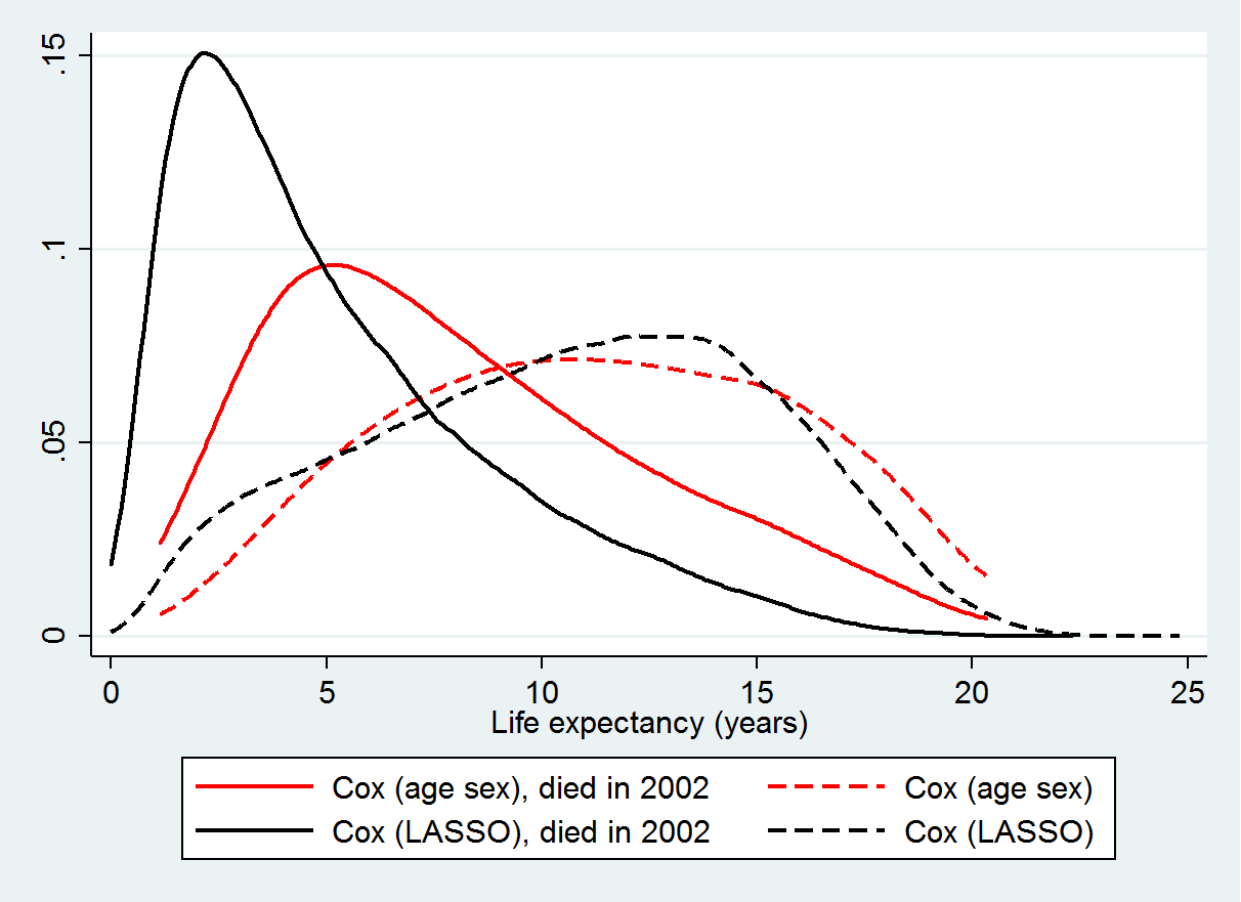

Appendix Figure A5. Kernel density plot of life expectancy estimates for Medicare beneficiaries alive on January 1, 2002. The dashed lines display the distributions of life expectancy for all Medicare beneficiaries alive on January 1, 2002. The solid lines limit the distribution to the subset of those beneficiaries who later died during the 2002 calendar year. The red lines display estimates from a Cox proportional hazards model that includes only age and gender as regressors. The black lines display estimates generated by estimating model (A3) using LASSO with 1,062 regressors.

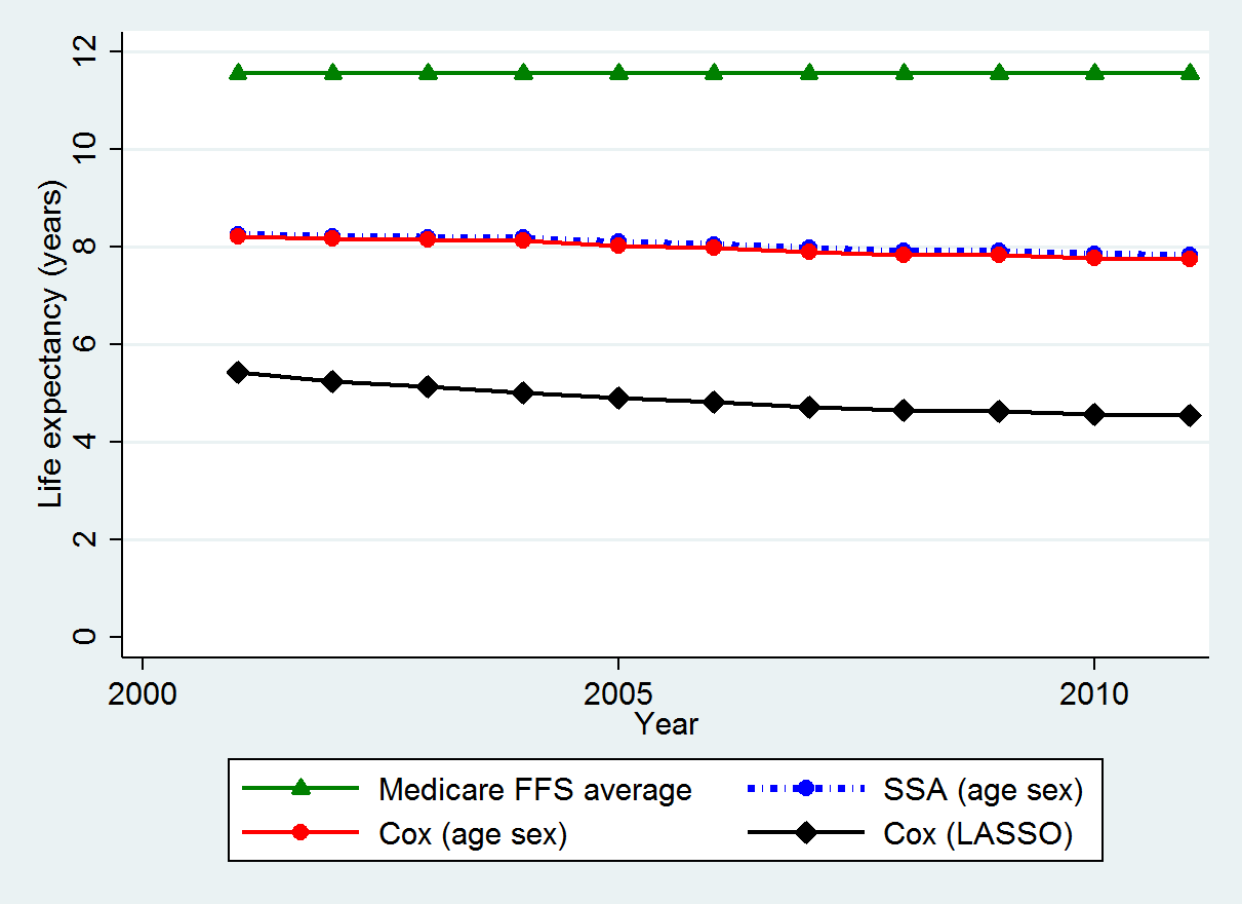

Appendix Figure A6. Average ex ante life expectancy for Medicare fee-for-service beneficiaries who later die within one year, by year. Estimates for "Medicare FFS average" are produced by estimating (A1) with no covariates. Estimates for "Cox (age sex)" are produced by estimating (A1) using only age and gender as predictors. Estimates for "Cox (LASSO)" are produced by estimating (A3) with 1,062 included regressors. Estimates for "SSA (age sex)" are obtained from the 2011 period life table for the Social Security area population (source: https://www.ssa.gov/oact/STATS/table4c6.html, accessed August 7, 2015).

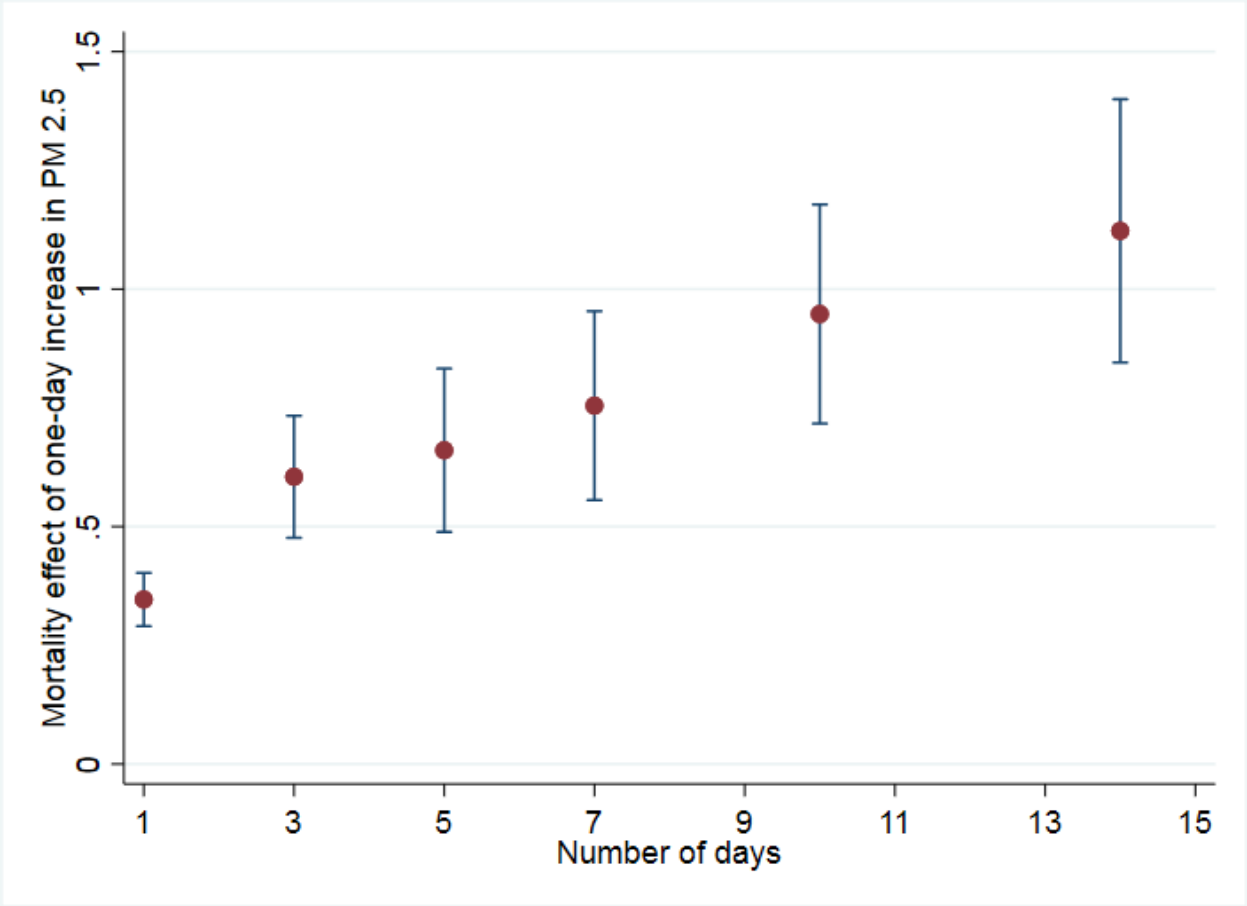

Appendix Figure A7. Mortality effect of one-day increase in fine particulate matter (PM 2.5) over longer time periods. Dependent variable is the mortality rate per million beneficiaries over the number of days indicated on the x-axis. PM 2.5 is instrumented for using daily wind direction, as described in the main text. All regressions include county, month-by-year, and state-by-month fixed effects; two lags of the instrument; flexible controls for temperatures, precipitation, and wind speed; and the appropriate number of leads of these weather controls and instruments (number of days minus one). Estimates are weighted by the number of beneficiaries.

APPENDIX TABLES

Table A1: Additional IV estimates of effect of PM 2.5

	(1) 1-day mortality, 75+ year olds	(2) 3-day mortality, 75+ year olds	(3) Same-day ER admissions rate
PM 2.5 ($\mu g/m^3$)	0.560***	0.930***	1.144***
	(0.063)	(0.111)	(0.156)
Effect of 10 $\mu g/m^3$ increase in PM 2.5, as percent of daily mean	2.734	4.544	1.924
F-statistic	248	248	237
Observations	1,600,846	1,600,846	1,518,549

Significance levels: * 10 percent, ** 5 percent, *** 1 percent. Table reports IV estimates of equation (1) from the main text. Standard errors (in parentheses) clustered by county. Dependent variable is shown in the column heading. All regressions include county, month-by-year, and state-by-month fixed effects, as well as flexible controls for temperatures, precipitation, and wind speed; two leads of the weather controls; and two leads and lags of the instruments. Estimates are weighted by the relevant population.

Table A2: IV estimates of effect of PM 2.5 on same-day mortality when controlling for other pollutants

	(1)	(2)	(3)	(4)	(5)
			Panel A: all beneficiaries		
PM 2.5 ($\mu g/m^3$)	0.266***	0.224***	0.239***	0.268***	0.209***
	(0.042)	(0.045)	(0.073)	(0.076)	(0.073)
Carbon monoxide		0.007**	0.008**	0.006*	0.007**
		(0.003)	(0.004)	(0.004)	(0.003)
Nitrogen dioxide			-0.041	-0.041	-0.105
			(0.141)	(0.135)	(0.140)
Ozone				-0.055	-0.052
				(0.063)	(0.061)
Sulfur dioxide					0.395**
					(0.182)
F-statistic	85	22	15	14	14
Dep. var. mean	132	132	132	132	132
Observations	333,903	333,903	333,903	333,903	333,903
			Panel B: fee-for-service beneficiaries		
PM 2.5 ($\mu g/m^3$)	0.367***	0.380***	0.385***	0.466***	0.397***
	(0.062)	(0.069)	(0.118)	(0.124)	(0.118)
Carbon monoxide		-0.002	-0.001	-0.004	-0.003
		(0.004)	(0.006)	(0.006)	(0.005)
Nitrogen dioxide			-0.016	-0.035	-0.133
			(0.222)	(0.208)	(0.225)
Ozone				-0.136	-0.135
				(0.092)	(0.088)
Sulfur dioxide					0.524*
					(0.273)
F-statistic	81	21	15	14	13
Dep. var. mean	156	156	156	156	156
Observations	293,973	293,973	293,973	293,973	293,973

Significance levels: * 10 percent, ** 5 percent, *** 1 percent. Standard errors (in parentheses) clustered by county. Table reports IV estimates of equation (1) from the main text, with the addition of the endogenous variables carbon monoxide, sulfur dioxide, nitrogen dioxide, and/or ozone, which are instrumented for using wind direction. Dependent variable is the 1-day mortality rate per million beneficiaries (Panel A) or per million fee-for-service (FFS) beneficiaries (Panel B). The sample is restricted to county-days where readings for carbon monixide, ozone, sulfur dioxide, nitrogen dioxide, and PM 2.5 are simultaneously available. All regressions include county, month-by-year, and state-by-month fixed effects; flexible controls for temperatures, precipitation, and wind speed; two leads of the weather controls; and two leads and lags of the instruments. Estimates are weighted by the number of Medicare beneficiaries in Panel A and by the number of FFS beneficiaries in Panel B.